ACS APPLIED MATERIALS & INTERFACES

RESEARCH ARTICLE

www.acsami.org

Phospholipid–Sepiolite Biomimetic Interfaces for the Immobilization of Enzymes

Bernd Wicklein, Margarita Darder, Pilar Aranda, and Eduardo Ruiz-Hitzky*

Instituto de Ciencia de Materiales de Madrid, CSIC, Cantoblanco, 28049 Madrid, Spain

Supporting Information

ABSTRACT: Biomimetic interfaces based on phosphatidylcholine (PC) assembled to the natural silicate sepiolite were prepared for the stable immobilization of the urease and cholesterol oxidase enzymes. This is an important issue in practical advanced applications such as biocatalysis or biosensing. The supported lipid bilayer (BL-PC), prepared from PC adsorption, was used for immobilization of enzymes and the resulting biomimetic systems were compared to several other supported layers including a lipid monolayer (ML-PC), a mixed phosphatidylcholine/octyl-galactoside layer (PC-OGal), a cetyltrimethylammonium monolayer (CTA), and also to the bare sepiolite surface. Interfacial characteristics of these layers were investigated with a focus on layer packing density, hydrophilicity/hydrophobicity, and surface charge, which are being considered as key points for enzyme immobilization and stabilization of their biological activity. Cytoplasmic urease and membrane-bound cholesterol oxidase, which served as model enzymes, were immobilized on the different PC-based hybrid materials to probe their biomimetic character. Enzymatic activity was assessed by cyclic voltammetry and UV–vis spectrophotometry. The resulting enzyme/bio-organoclay hybrids were applied as active phase of a voltammetric urea biosensor and cholesterol bioreactor, respectively. Urease supported on sepiolite/BL-PC proved to maintain its enzymatic activity over several months while immobilized cholesterol oxidase demonstrated high reusability as biocatalyst. The results emphasize the good preservation of bioactivity due to the accommodation of the enzymatic system within the biomimetic lipid interface on sepiolite.

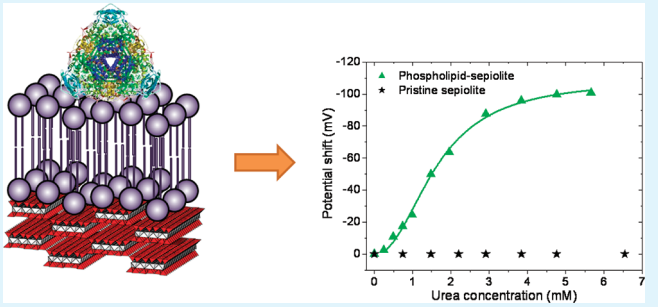

KEYWORDS: phospholipid, sepiolite, clays, enzymes, cellular membrane, biomimetic interface, biohybrid materials

INTRODUCTION

Enzymes are a group of functional proteins with the ability to catalyze specific reactions.[1] This property has been widely exploited in advanced devices such as biosensors, bioreactors,[1] or in enzymatic fuel cells.[2] Economic reasons demand reusability, long shelf-life time, and efficient usage of the applied enzymes. Therefore, immobilization on solid supports is mandatory to match these requirements and consequently, numerous strategies have been developed over the past decades.[3−13] However, many enzyme-hybrid complexes may suffer from leaching, and degradation could not always be sufficiently reduced, especially at extended self-lifetime.

The challenge in immobilization of enzymes is to provide sufficient linkages as necessary to prevent enzyme leaching but at the same time accommodating these proteins as gently as possible to avoid loss of bioactivity. Therefore, one of the most promising routes to solve these problems is to immobilize enzymes in environments as similar as possible to biological systems. This concept of biomimetism is based on the inspiration by naturally occurring structures and tries to replicate them for the use in advanced applications.[14,15]An interesting approach herein comprises bioinspired interfaces which are especially advantageous for bioelectrode applications.[16−18] This strategy involves molecular modification of a solid surface with biological species as for instance lipids, giving rise to the well-studied systems of the supported artificial lipid cell membranes.[19−21] Biomimetic lipid membranes are ideal host matrices for the maintenance and transduction of enzymatic activity.[22]

For efficient and sensitive biocatalysis and biosensing, a large contact interface between the substrate bulk solution and the supported bioactive phase is important. Therefore, controlled formation of lipid membranes on large specific surface area materials has been described, e.g., on silica,[23] layered silicates,[24] or layered double hydroxides.[25] These works indicated versatile routes to increase lipid membrane surface area for enhanced loading of biological species.

Recently, we reported the preparation of a new type of bionanohybrid materials based on lipid modified clay minerals.[26,27] Clay minerals are large surface materials and display various types of external and internal surfaces that are generally viable to modify.[28]

Received: July 29, 2011
Accepted: October 4, 2011
Published: October 04, 2011

dx.doi.org/10.1021/am201000k | *ACS Appl. Mater. Interfaces* 2011, 3, 4339–4348

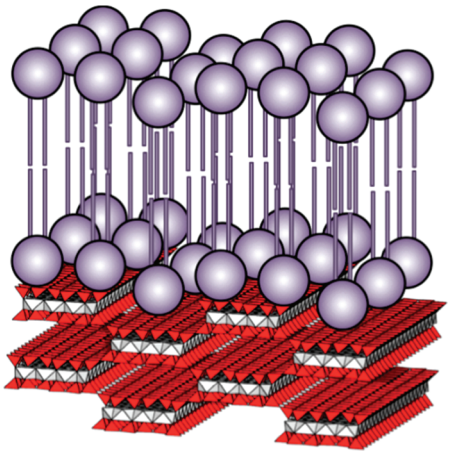

Figure 1. Schematic representation of a bilayer lipid membrane assembled on the external surface of a sepiolite fiber.

The bionanohybrids in this work are composed of the fibrous magnesium silicate sepiolite as solid support for the artificial lipid membrane (Figure 1). The molecular adsorption from organic solvent permits feasible control over the deposition of lipid mono- or bilayer assemblies.

In the present communication, bioinspired interfaces of different physicochemical properties, including a lipid mono- and bilayer, a mixed lipid/sugar surfactant layer, and a monolayer of the long-chain alkylammonium detergent cetyltrimethylammonium bromide are studied as immobilization hosts for enzymes to probe their biomimetic and biocompatible nature. Therefore, the association of two different kinds of enzymes, urease (URE) and cholesterol oxidase (COx), was carried out. Urease is a cytosolic enzyme that is present in cells of many plants, bacteria, fungi, and algae.[29] Cholesterol oxidase, on the other hand, is a membrane-bound flavoenzyme that catalyzes the oxidation and isomerization of cholesterol to cholest-5-en-3-one[30] and is related to coronary heart diseases, arteriosclerosis, cerebral thrombosis, and miscellaneous other dysfunctions.[31] The choice of these enzymes reflects two general schemes of enzyme association to membranes: external and intrinsic association. The first one is often adopted by cytosolic enzymes, whereas the latter is frequently found for membrane-bound enzymes presenting a hydrophobic side chain for insertion into the lipid membrane.

The adsorption mechanism of URE and COx on the various interfaces is here investigated and compared in terms of the individual physicochemical properties such as layer packing density, surface groups, and surface potential. The catalytic activity of the immobilized enzymes was assessed by cyclic voltammetry as well as by UV−vis spectrophotometry. The resultant enzyme/bio-organoclay hybrids were tested as active phase of a voltammetric urea biosensor and as cholesterol bioreactor.

MATERIALS AND METHODS

Starting Materials and Reagents. Sepiolite (SEP) from Vallecas, Madrid (Spain) of >95% purity commercialized as Pangel S9 with a cation exchange capacity close to 15 mequiv/100 g and a BET (N_2) specific surface area of 310 m^2/g was furnished by TOLSA and used as supplied. Phospholipids from soybean of 92% L-α-phosphatidylcholine (PC) content commercialized as Emulmetik 930 were kindly provided as a gift from Lucas Meyer Cosmetics and used as received.

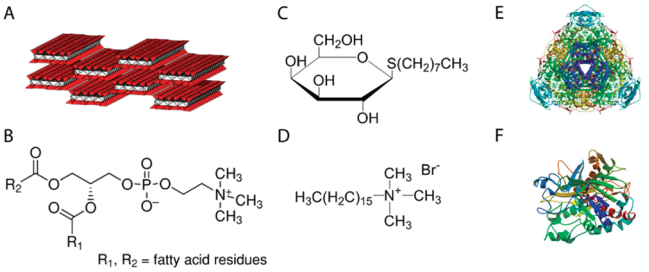

Figure 2. Schematic representations of the (A) sepiolite structure and the molecular structures of (B) phosphatidylcholine (PC), (C) n-octyl-β-D-galactoside (OGal), (D) cetyltrimethylammonium bromide (CTAB), (E) Jack Bean urease (URE), and (F) cholesterol oxidase (COx). The compound dimensions are not proportional for the sake of visualization.

Among the 8% in weight are lipids belonging to the lyso family as well as phosphorus compounds and moisture. Urease (URE) from *Canavalia ensiformis* (Jack Bean) with 50590 u/g solid and cholesterol oxidase (COx) from *Brevibacterium sp*. with 28 u/mg solid, as well as cetyltrimethylammonium bromide (CTAB) were purchased from SigmaAldrich. n-Octyl-β-D-galactoside (OGal) was delivered by Carbosynth. See Figure 2 for the structures of these materials. Albumin from bovine serum (BSA), urea (≥98%), cholesterol (≥98%), and Triton X-100 were purchased from Sigma. Coomassie Brilliant Blue G was supplied by Aldrich. 5,5′-Dithiobis(2-nitrobenzoic acid) (DTNB) was received from Fluka. 2,2′-Azino-bis(3-ethylbenzthiazoline-6-sulfonic acid) (ABTS), peroxidase from horseradish (HRP) and KH_2PO_4 were obtained from SigmaAldrich. Isopropanol and ethanol were of synthesis grade. Deionized water (resistivity >18.2 MΩ cm) was used throughout this work and obtained from a Maxima Ultrapure Water system from Elga.

Biohybrid Synthesis Procedure. The synthesis of the sepiolite-lipid biohybrids is described elsewhere in detail.[26] In short, phospholipid is dissolved in ethanol at a concentration of 2.5 or 13.5 mM to obtain a supported ML-PC or BL-PC. The sepiolite concentration was fixed to 0.2 wt %. The suspensions were stirred for 24 h at ambient temperature (approximately 22 °C). The resultant biohybrids were collected by centrifugation (8000 rpm, 15 min.), vacuum-dried at room temperature and ground to powder for further usage. As PC is considered as the main adsorbate from phospholipid solutions the obtained materials are henceforth designated as S-PC including ML and BL. The mixed PC-OGal layer was obtained from adsorption of OGal on a previously formed PC monolayer on sepiolite (S-ML-PC). For the OGal adsorption isotherm 0.2 wt % S-ML-PC were suspended in an aqueous solution of OGal with concentrations between 0.078 and 5 mM. The suspension was stirred at ambient temperature for 24 h. OGal adsorption was estimated from the OGal concentration in the supernatant and determined with the phenol-sulfuric acid method.[32] The preparation of sepiolite-cetyltrimethylammonium (S-CTA) has been described elsewhere.[33]

Enzyme Immobilization. Enzyme immobilization for the activity assays took place in 50 mM phosphate buffer (PB) solution at pH 7 with 0.3 wt% adsorbent material dispersed. Enzyme stock solutions were prepared in 50 mM PB at pH 7 with 1 mg/mL URE or 2 mg/mL COx. The enzyme concentration in the adsorption suspension was fixed to 1 mg/mL for URE and 0.125 mg/mL for COx. The incubation time was 2 h at ambient temperature (22 °C) under gentle agitation on a magnetic stirrer. Adsorbents were separated by centrifugation. Enzyme adsorption quantities were determined from the supernatant following the Bradford total protein assay[34] using BSA as reference and utilizing a Shimadzu UV-2401 PC UV−vis spectrophotometer.

Characterization. Surface characteristics of S-PC-OGal hybrids were investigated by sampling water adsorption isotherms at 25 °C, in the range of relative humidity between 0 and 95%, with a Gravimetric water sorption analyzer (Aquadyne DVS) from Quantachrome Instruments (FL, USA). Prior to measurements, the samples were purged at 80 °C until the sample weight remained constant. Fourier transform infrared (FTIR) spectra were recorded on a Bruker IFS 66v/S Spectrometer with 2 cm^{-1} resolution. The samples were prepared as self-standing films and measured in transmission mode ζ-potential measurements of 0.05 wt % suspensions in 50 mM PB (pH 7.0) were performed on a Malvern Zetasizer Nano ZS.

Reagentless pH Sensor for Urease Activity Assays. The reagentless pH probe was based on polycrystalline gold disk electrodes, which were conditioned and modified with a self-assembled monolayer of 5,5′-dithiobis(2-nitrobenzoic acid) (DTNB) as reported elsewhere.[35] Holding the potential at −0.53 V for 3 s triggers the generation of a reversible, surface-confined NHOH/NO redox couple with a formal potential of 0.035 V vs Ag/AgCl. This redox couple is pH dependent resulting in a corresponding peak potential shift as the pH value at the electrode surface changes due to the enzymatic reaction. Thus, the DTNB modified gold electrode can be used as a reagentless voltammetric pH sensor, based on the following relationship: E_p = 0.453−0.059 pH (see the Supporting Information S1). For measurement of enzymatic activity, urease-biohybrids were deposited as films by a 10 μL drop on the DTNB modified gold electrode surface from a PVA suspension (0.5 wt %) containing 1 wt.% URE-biohybrid and allowed to dry at ambient temperature. CV measurements were carried out with a minipotentiostat μSTAT 100 from DropSens in 10 mM PB (pH 7.4) with a typical three electrode setup consisting of the surface modified gold electrode, a platinum auxiliary electrode and a Ag/AgCl reference electrode. The potential range was set to +0.2 and −0.3 V with a scan rate of 50 mV/s. Prior to use, the electrodes were conditioned in PB for 30 min to ensure sufficiently well-hydrated films. Urea aliquots were added from a 0.1 M standard stock solution that was prepared weekly and stored at 4 °C.

COx Activity Assays. COx activity was deduced from measuring H_2O_2 oxidation current with a platinum wire as working electrode (three electrodes setup with Pt auxiliary electrode and Ag/AgCl reference electrode) in suspension with 0.5 wt % COx-biohybrid dispersed. The supporting electrolyte was 50 mM PB at pH 7.5. Cholesterol stock solutions of 0.1 M in isopropanol were prepared freshly prior to use. Cholesterol working solutions of 0.25 mM were prepared from 50 mM PB (pH 7.0) containing 1 wt %. Triton X-100 by adding an aliquot of cholesterol stock solution under vigorous stirring and then warmed up slowly to 60 °C until the solution becomes clear. CV was conducted between 0 and +0.65 V with 50 mV/s and H_2O_2 was detected at +0.6 V.

COx-Bioreactor Preparation. COx-bioreactors were prepared with the supports S-ML-PC and S-BL-PC, respectively. The COx enzyme was immobilized from a 2000 μg/mL stock solution by contacting 3 mg support with 160 μg COx. After 2 h incubation at ambient temperature the solid was separated and washed with copious amounts of PB.

Enzymatic activity of COx-bioreactors was determined from spectrophotometric experiments. Cholesterol working solutions of 0.5 mM in PB were prepared as described above. The bioreactor (3 mg) was suspended in 2 mL PB and an aliquot of cholesterol working solution was added. The mixture was thermostatted for 7 min at 25 °C in a water bath shaker. The solid was then separated by centrifugation and the supernatant was analyzed for the amount of enzymatically produced H_2O_2 using a Shimadzu UV-2401 PC UV−vis spectrophotometer. Therefore, 1 mL of supernatant was mixed with 10 μL of 10 mM ABTS and 50 μL of 23 μM HRP and brought up to 2 mL with PB. After 2 min a UV−vis spectrum was collected and the absorbance at 728 nm was measured. The recyclability of bioreactors was also evaluated. After each addition of 31 μM cholesterol, the activity assay was conducted as described above. The supported enzymes were separated and washed thoroughly in PB before starting a new catalysis cycle.

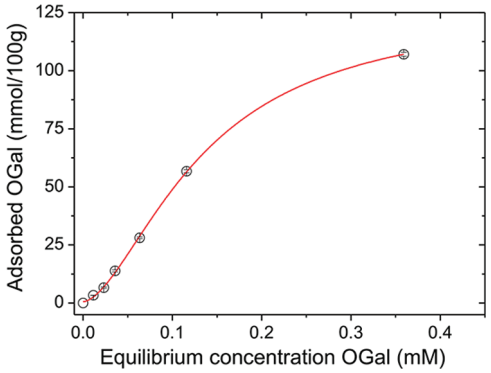

Figure 3. Adsorption isotherm of OGal on S-ML-PC obtained in water at 21 °C. The solid line represents the fitting curve of a logistic growth model (R^2 = 0.9997).

RESULTS AND DISCUSSION

Surface Properties of Sepiolite-Hybrid Materials. Pristine sepiolite and modified sepiolite with different interfacial properties were prepared and compared in terms of enzyme immobilization performance. Sepiolite with hydrophobic surface modification was obtained by PC and CTA monolayer formation, respectively. Hydrophilic surface layers were provided by PC bilayers and mixed PC-OGal layers, respectively.

The neat sepiolite used in this work was reported to have an isoelectric point (iep) of 2.2−3.3.[36] Consequently, the observed ζ-potential at pH 7 in 50 mM PB is −27.8 ± 0.3 mV. The negative surface charge is accounted to Mg^{2+} by Al^{3+} isomorphous substitutions in the octahedral layers giving rise to cation exchange behavior, typically in the 15−20 mequiv/100 g range.[37] Another suggested origin of the negative surface charge was attributed to the presence of −Si−O^- groups, originating from deprotonation of surface hydroxyl groups and adsorption of OH^- ions.[38]

According to the previously described procedure[26] a PC monolayer with 25 mmol/100 g was formed on sepiolite, yielding a packing density of 0.92 lipid molecules per nm^2. The ζ-potential of the S-ML-PC hybrid decreased to −18.5 ± 0.7 mV. Similar observations were made in the silica liposome system.[39,40] This decrease in ζ-potential has been attributed to a shielding effect imposed on the surface charge by adsorbed PC molecules. As a result, PC shifts the electrokinetic slip plane outward and thus, decreasing the absolute value of the ζ-potential. The sepiolite supported lipid bilayer[26] has a ζ-potential of −18.1 ± 0.7 mV and contained 50 mmol/100 g, revealing a molecular density of 0.92 lipids/nm^2 in each membrane leaflet, which indicates the exact complement of the monolayer. Packing density, however, is somewhat lower than in PC liposomes or supported bilayer lipid membranes on even surfaces.[41] This may well be ascribed to irregularities of the fiber surface giving rise to microroughness which can be a reason for the reduced layer packing density. Actually, the position of the asymmetric CH_2 IR band of organic molecules can be used to study the compaction of self-assembled monolayers on smooth surfaces (e.g., gold).[42] In the present case, an insignificant peak shift of 3 cm^{-1} has been

observed for increasing PC content on sepiolite (data not shown). This is therefore in agreement with the lower packing density of the PC layers on sepiolite.

Layer formation of OGal was investigated by sampling the adsorption isotherm of this biosurfactant on S-ML-PC which followed a sigmoidal shape (Figure 3).

This type of adsorption isotherm is typical for adsorbates that show intermolecular cooperativity based on van der Waals interaction between hydrophobic moieties.[43] In particular, nonionic surfactants have been observed to adsorb at hydrophobic solid/water interfaces in this manner.[44] The saturation level is calculated as 127 mmol/100 g, which corresponds to a molecular packing density of 4.7 OGal molecules per nm^2. This is about 2 times the monolayer packing density of n-octyl-β-D-glucoside at the air/water interface.[45] It is assumed that the PC monolayer serves as anchor and nucleation site for the growth of the OGal outer membrane leaflet by hydrophobic interaction between the hydrocarbon chains.[46] This assumption is also supported by Persson et al.,[47] who investigated the adsorption of n-dodecyl-β-D-maltoside on hydrophobized surfaces based on silane and concluded insertion of alkyl chains of the sugar-based surfactant into the hydrophobic silane layer as anchoring mechanism. The excess of OGal might be explained in terms of hydrophobic aggregation or hemimicelle formation,[48,49] which can occur even at surfactant concentrations considerably below the critical micelle concentration.[50] In consequence, this can lead to increased molecule packing density and might explain in the present case the elevated packing density of OGal on the PC monolayer. On the other hand, this packing density value could equally well be achieved by assuming the formation of an OGal bilayer. However, hydration repulsion between the headgroups of sugar-based surfactants is known to occur,[51] and hence, would impede the assembly of an OGal bilayer in this fashion.

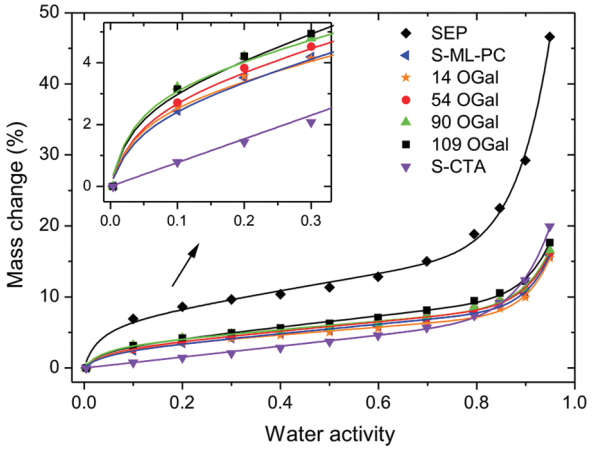

Figure 4. Water adsorption isotherms at 25 °C for pristine sepiolite (SEP), S-CTA, S-ML-PC and S-PC-OGal hybrids containing 14, 54, 90, and 109 mmol/100 g of OGal. The solid lines are calculated from Park's equation. The inset shows the regime of Langmuir adsorption.

The alteration of surface hydrophilicity upon OGal adsorption was studied by sampling water adsorption isotherms on the prepared S-PC-OGal biohybrids. Figure 4 displays the water adsorption isotherms on pristine sepiolite, S-ML-PC and S-PC-OGal with increasing OGal content. All the tested materials show isotherms with a sigmoidal shape which is characteristic of hydrophilic materials. The isotherms were analyzed according to the Park's model,[52] rendering the Langmuir capacity constant A_l (water monolayer coverage) from the initial slope of the curves which can be interpreted as measure for hydrophilicity of the exposed interface. The high A_l value of 6.9 g/100 g confirms the hydrophilic behavior of pristine sepiolite fibers. After adsorption of a PC monolayer, A_l is considerably reduced (2.5 g/100 g), but the successive increase of OGal quantities at the ML-PC surface gave rise to gradually increasing A_l values until 3.6 g/100 g. This behavior is attributed to the elevated presence of hydrophilic galactoside groups at the external surface. A more detailed discussion on the obtained isotherm fitting parameters is provided in the Supporting Information S2. The measurement of the ζ-potential of S-PC-OGal (109 mmol/100 g) revealed -21.6 ± 1.3 mV, which remains close to the value of the lipid monolayer. This was expected because the adsorption of a nonionic compound imposes only little alteration on the ζ-potential.[46]

The surface properties of S-CTA are characterized with the intention to provide a comparison between the monolayers of the biosurfactant PC and the organo-surfactant CTA. This can be of importance for subsequent studies related to the association of biological species on these materials. CTA adsorption on sepiolite yielded 34 mmol/100 g, which results in a packing density of 1.25 molecules/nm^2 (or 0.8 nm^2/molecule). This value is higher than the cross-section area of 0.5 nm^2 of a CTAB molecule in a monolayer on silicon dioxide.[53] The microscopic roughness of sepiolite may reduce the ideal packing density of the CTA monolayer. However, according to water sorption (Figure 4), the CTA monolayer is significantly more hydrophobic than the PC monolayer. This suggests denser molecule packing than in the case of the ML-PC. In this last case, the kink attributable to the double bond in the acyl chain of the PC molecule impedes the same high degree of ordering and allows for partial penetration of water molecules into the layer. Adsorption of the cationic CTA$^+$ changed the ζ-potential of sepiolite to a value close to zero. This surface charge compensation indicates Coulomb interactions between CTA$^+$ and the negative charge sites on sepiolite together with a shielding effect of organized paraffin chains. Table 1 reports the discussed surface properties.

Enzyme Adsorption on Different Sepiolite Surfaces. Urease was adsorbed on neat sepiolite and the different hybrid materials from PB at pH 7.0. Figure 5 shows the uptake of urease from where it can be seen that any kind of surface modification enhanced urease retention with respect to pristine sepiolite.

It is very complex to ascertain the predominant type of interaction between URE and the support as electrostatic and hydrophobic forces, both from different protein residues and the involved particular surfaces, may contribute in different extend to the overall adsorption process in each case. For instance, pristine

Table 1. Overview of Layer Properties and ζ-Potential Values

	SEP	ML-PC	CTA	BL-PC	PC-OGal
ads. quantities (mmol/100 g)		25	34	50	25 + 109
molecule density (nm^{-2})		0.73	1.25	1.46	4.70
ζ-potential (mV)	-27.8 ± 0.3	-18.5 ± 0.7	-3.7 ± 0.3	-18.1 ± 0.7	-21.6 ± 1.3

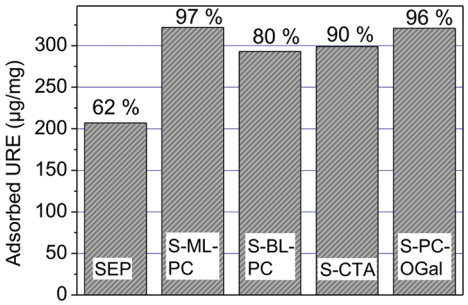

Figure 5. Urease adsorption on bare sepiolite and sepiolite hybrid materials with urease uptake given in percentage of available enzyme quantity.

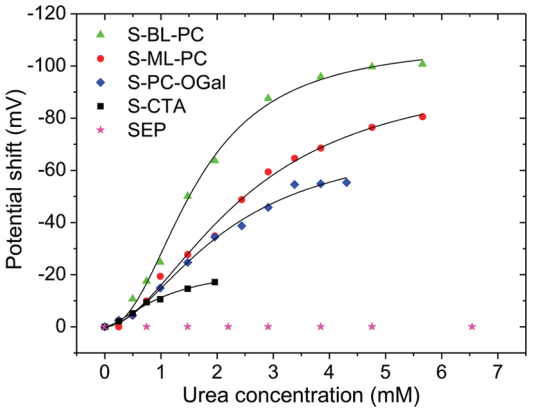

Figure 6. Potential shift of DTNB as a result of pH increase produced by urea oxidation and plotted as function of urea concentration. The solid lines represent the fitting curves to the Hill model. Urease was immobilized on pristine surface and sepiolite displaying biointerfaces such as BL-PC, ML-PC, PC-OGal, and CTA.

sepiolite and S-BL-PC display ionic interaction sites like negatively charged centers on the clay surface and trimethyl ammonium and phosphatidyl groups of the lipid molecules. Moreover, the ζ-potential of both materials is negative (sepiolite, −27 mV; S-BL-PC, −18 mV). However, under the conditions of immobilization (pH 7.0) the surface of URE is negatively charged (isoelectric point (i_{ep}) of urease is 5.0−5.2)[54] and ionic repulsion is likely to counteract attractive forces and consequently, reduce adsorption quantities. On the other hand, attractive forces might be, in case of S-BL-PC, H-bonding between the lipid headgroup and cysteine, tyrosine, or histidine side chains of URE. Additionally, glutamate, present in URE,[55] is known to strongly interact electrostatically with the phosphatidylcholine headgroup.[56]

Urease adsorption on S-PC-OGal (109 mmol OGal/100 g) yielded very high retention. This can be attributed to the very polar headgroup of OGal, comprising four slightly acidic hydroxyl groups (pK_a 12.35)[57] and two etheric oxygen atoms. These are prone to form dipole−dipole and even dipole-ion interactions with the polar and ionic regions of the urease surface. Also H-bonding with urease side chains cysteine, tyrosine, or histidine is likely to occur. Together, these interactions are supposedly strong enough to compensate for the ionic repulsion between the anionic URE and S-PC-OGal.

High adsorption quantities were also determined on the hydrophobic PC and CTA monolayers. On urease a large hydrophobic patch is surrounding the binuclear nickel catalyst center[58] that may well interact and adsorb on hydrophobic surfaces.[59] This might explain the observed high retention of this enzyme.

Adsorption of the membrane-bound enzyme cholesterol oxidase (COx) on the different interfaces was also assessed and it was found to be equally high for all tested materials. Enzyme concentration in the supernatant was below detection limit of the total protein assay and gave an uptake of ca. 45 µg/mg corresponding to a 100% uptake of all available enzyme

The iep of COx is around 4.7 (Supplier data), which renders the COx surface negative at the pH value used in the immobilization step. However, attractive interactions are apparently stronger. Sampson et al.[60] observed COx binding constants to vary only little with membrane surface charge, ionic strength, or pH which suggests that surface binding to membranes is mainly driven by hydrophobic interaction. This may explain the equally high retention on different type of interfaces such as lipid layers, CTA membrane, or pristine sepiolite. The high retention of COx on pristine sepiolite in contrast to the lower adsorption of URE might be attributed to entrapment in microcavities, probably most in the mesopores of the clay fibers. The COx protein has a molecular mass of 64 kDa, with a molecular cross section of

Table 2. Activity of Immobilized Urease As Indicated by the Slope of the Potential Shift As Function of Substrate Concentration[a]

	interface				
	SEP	ML-PC	BL-PC	CTA	PC-OGal
slope (VM^{-1})	0	−21.3	−33.3	−10.2	−16.8
I_{max} (mV)		−99.8	−109.0	−23.9	−73.3
$[C_{0.5}]$ (mM)		2.5	1.62	1.1	2.1
$\lvert I_{max}/[C_{0.5}]\rvert$ (VM^{-1})		39.9	67.3	21.7	34.9

[a] The kinetic parameters I_{max} and $[C_{0.5}]$ as well as the catalytic efficiency $I_{max}/[C_{0.5}]$ are derived from fitting to the Hill model.

15 nm^2 according to Wildgoose et al.,[61] which is smaller than URE (460 kDa) and might therefore easily enter the microcavities.

Enzyme Activity Measurements and Immobilization Mechanism. *Urease.* Kinetics of immobilized urease were assessed electrochemically by means of a reagentless voltammetric pH probe[62,63] based on the redox compound DTNB assembled to the gold electrode surface. As detailed in Supporting Information S1, the redox signal due to the couple NHOH/NO derived from DTNB is shifted toward more negative potential values as pH increases. Thus, this potential shift is useful to detect the increase of pH as result of the catalyzed oxidation of urea (eq 1):

$$(NH_2)_2CO + 3H_2O \rightarrow 2NH_4^+ + HCO_3^- + OH^- \quad (1)$$

The produced peak shift was plotted as a function of the urea concentration in the supporting electrolyte (Figure 6). The linear slope of the curves provides a measure for the preserved enzymatic activity on the different interfaces (Table 2). Because of the sigmoidal curve shape, the data was fitted to the Hill model[64] for kinetic evaluation of the immobilized enzyme

$$I = \frac{([C]/[C_{0.5}])^h}{1 + ([C]/[C_{0.5}])^h} I_{max} \quad (2)$$

where I_{max} is the maximum rate of the enzymatic reaction, $[C_{0.5}]$ is the concentration at half saturation, and h is the Hill coefficient.

Table 3. Analytic and Kinetic Parameters for COx Immobilized on Different Surfaces

	interface					
	SEP	S-ML-PC	S-BL-PC	S-CTA	S-PC-OGal	Free COx
sensitivity (mA M^{-1})	62	154	138	0	24	47
linear range (μM)	up to 4.9	up to 4.9	up to 3.7		2.5−4.9	up to 4.9
K_M^{app}	2.1	5.0	4.4		8.7	8.8
I_{max}	0.43	1.31	1.10		0.26	0.65

Lipid containing interfaces provide high urease activity with the lipid bilayer having the highest of all studied interfaces. The good maintenance of bioactivity on this material may be ascribed to the close resemblance of the supported lipid bilayer to biological lipid structures and thus, providing optimal immobilization conditions. This is also reflected by the high catalytic efficiency $I_{max}/[C_{0.5}]$ (Table 2). Pristine sepiolite, on the other hand, did not conserve enzymatic activity at all. This could be attributed to the fact, that catalytic activity may be compromised due to interaction with the support. The IR amide I and II bands of the amino acid chains can provide indications of the state of protein structure deformation caused by strong support−enzyme interaction or by degradation processes. On pristine sepiolite, for instance, immobilized urease showed a significantly perturbed amide II band appearing at 1521 cm^{-1}, indicating at least a partial denaturation of the immobilized enzyme (see the Supporting Information, Figure S3). For the other materials, FTIR spectra showed no signs of band perturbation which indicates maintenance of the enzyme conformation, even though the band was in some cases extremely weak. Unfortunately, the stronger amide I band is superimposed by the OH band of water molecules adsorbed on sepiolite. The inconstancy of the OH band upon adsorption of organic species prevents a subtraction of this band for deconvolution of the amide I band and therefore cannot be used for assessment of the protein structure.

On the CTA interface, a high amount of urease was adsorbed but the sample demonstrated low activity and catalytic efficiency. This may be explained in terms of protein orientation and hydrophobic interactions. As explained earlier, urease possesses a large hydrophobic patch surrounding the Ni catalyst center. Hydrophobic interaction with the CTA interface is likely to orientate the enzyme with its catalyst center toward the support surface and hence, hampering the access of urea to the catalyst site. Additionally, it can be assumed that CTA-protein interactions caused protein structure distortion analogously to the URE-palmityl glycidyl ether system in which case protein unfolding occurred,[65] even though in the present case no direct evidence could be retrieved from IR examination.

Similar interactions may apply in case of S-ML-PC, however to a smaller extend. Here again, the activity is lower than for S-BL-PC. But the lower packing density as compared to the CTA monolayer and therewith accompanied higher membrane fluidity may allow the enzyme to reorientate and thus, recover some of its activity. This assumption is also supported by the significant long-term conservation of enzymatic activity on S-ML-PC over a period of several weeks (Supporting Information Figure S4). It indicates that the reduced activity is less related to hydrophobic induced degradation processes which eventually will decline the activity to zero, but rather to conformational obstructions. This long-term activity, for instance, was not observed for S-CTA.

Urease activity at the mixed PC−OGal interface is inferior to the lipid bilayer. Galactoside residues on the outer surface seem not to stabilize urease sufficiently. Nonionic sugar-based surfactants such as alkyl glucosides are known as versatile protein solubilizers under the avoidance of typical denaturation effects caused by many ionic detergents.[66] Enzyme activity was also reported to be unaffected by this class of mild detergents.[67] Therefore, this interface was initially presumed to be a good scaffold for sustainable enzyme immobilization. Instead, it might be reasonable to consider the different type of electrostatic interaction between OGal and URE as compared to PC as possible cause for the decayed activity. This result indicates the necessity of a fully developed lipid bilayer that truly mimics and acts as a biocompatible cellular membrane for optimal enzyme immobilization and activity.

For all cases, the Hill coefficient h was between 1.5 and 2, corroborating a deviation from classical Michaelis−Menten kinetics[64] as result of allosteric effects.[68]

Cholesterol Oxidase. The activity of immobilized COx was assessed by plotting calibration curves (Figure 7a) from the oxidation current response that originates from the H_2O_2 produced in the COx catalyzed reaction (eq 3)

$$\text{cholesterol} + O_2 \xrightarrow{\text{COx}} \text{cholest} - 4 - \text{en} - 3 - \text{one} + H_2O_2 \quad (3)$$

The deduced analytical parameters are listed in Table 3. Apparent kinetics of immobilized enzymes are determined among others by two factors: (1) enzyme structure degradation due to support−enzyme interactions and, (2) mass transport limitations both in the external bulk solution and the internal supporting matrix.[69] Fitting the obtained substrate conversion data to appropriate models may reveal these processes. Lineweaver−Burk plots (Figure 7b) were constructed from the reaction data to determine the apparent values of the Michaelis−Menten constant K_M^{app} and the maximum current I_{max}.

The linearity of the Lineweaver−Burk plots indicates the absence of mass transport restrictions[69,70] because of free substrate access to COx, which is adsorbed on the surface of the suspended hybrid materials. Furthermore, because all studied materials contained similar enzyme quantities according to the total protein assay all observed kinetic variations should be solely associated with variations in enzyme activity.

In this way, COx immobilized on S-ML-PC produced the largest response. The linear range and sensitivity were found to be 0−4.9 μM and 154 mA M^{-1}, respectively. Slightly inferior sensitivity was detected on S-BL-PC. The results demonstrate good immobilization at the lipid interfaces with even enhanced sensitivity in comparison to free COx. Reduced activity was detected on the mixed PC-OGal interface and on pristine sepiolite while no enzymatic activity was registered at the CTA

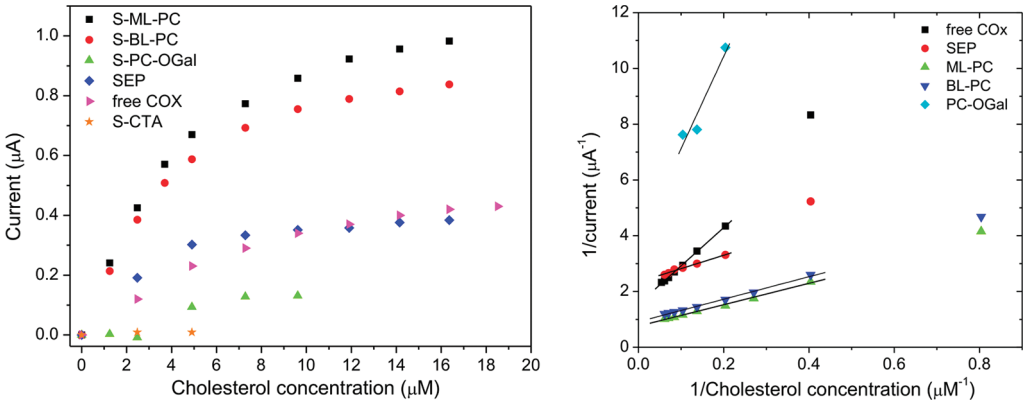

Figure 7. (a) Calibration plots of COx immobilized on sepiolite displaying biointerfaces such as BL-PC, ML-PC, mixed PC−OGal, CTA, and pristine surface. (b) Lineweaver−Burk plots were derived from the conversion data.

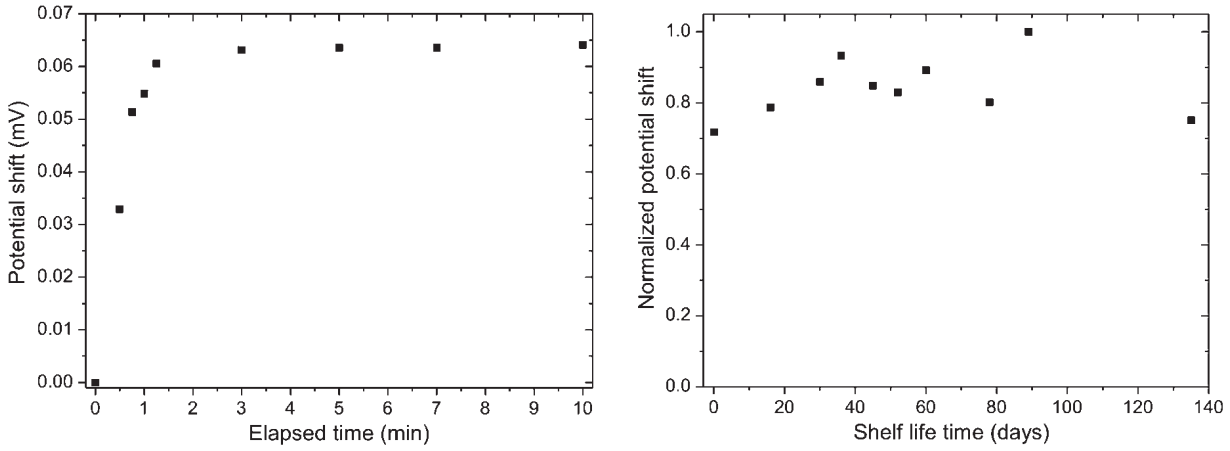

Figure 8. (a) Response time of urease-bioelectrode in 10 mM PB (pH 7.4). After addition of 4.8 mM urea the solution was 30s magnetically stirred and the time henceforth referred to as elapsed time. The produced peak shift was determined by CV (+0.2 to −0.25 V, 50 mV/s). (b) Shelf-life time of urease supported on S-BL-PC and stored as dry powder at 4 °C before usage. The potential shift was determined at 2 mM urea concentration with CV (+0.2 to −0.25 V, 50 mV/s) on a DTNB-modified Au electrode as described above.

interface. These findings were supported by the kinetic parameters obtained from Lineweaver−Burk plots. COx immobilized on both PC mono- and bilayer showed a decreased K_M^{app} of about 5.0 and 4.4 μM, respectively, when compared to free COx (8.8 μM). Immobilization at the PC-OGal interface rendered an apparent Michealis-Menten parameter in the range of free COx while pristine sepiolite provided the lowest K_M^{app} with 2.1 μM but also a very low I_{max} value (0.43 μA). Low K_M^{app} is indicative for fast kinetics and high substrate affinity. It is a frequently made observation that enzymes immobilized on adequate supports may show faster kinetics than the soluble, free enzyme.[71,72] Hence, it is obvious that S-BL-PC offered the best environment of all tested interfaces for COx immobilization. Also when comparing the long-term stability after four weeks, the K_M^{app} value from S-BL-PC was lower than from S-ML-PC (15 and 104 μM, respectively; see the Supporting Information, Figure S5). Both K_M^{app} increased (2.3-fold for S-BL-PC and 22.6-fold for S-ML-PC) because of slow protein denaturation, but the PC bilayer limited this fate to a significantly lower extent. Sampson et al.[60] could show that the amphiphathic active-site loop (residues 78−87) of COx interacts with the choline moiety of the lipid headgroup while amino acid chains of this loop insert ca. 0.8 nm into the cellular lipid bilayer to ensure an appropriate spatial orientation of the active center. We presume that this 2-fold specific interaction with the PC bilayer supported on sepiolite in the present case enables the high and long-lasting activity of COx. Contrarily, COx did not preserve any activity on the monolayer composed of CTA. Strong hydrophobic interaction between alkyl chains of CTA and the hydrophobic region of COx are possibly accounted for this observation. Additionally, COx amino acid chains are possibly hindered to penetrate into the membrane since the CTA monolayer is more densely packed. The mixed PC-OGal interface rendered diminished activity despite of its structural resemblance to the PC bilayer. Here, the amino acid chains are likely to insert with more ease because of the lower packing degree of the outer membrane leaflet. But on the other hand, electrostatic stabilization as with the choline moiety on a lipid bilayer is not possible.

Application of Enzyme-Supported Biohybrids. *Urease Biosensor.* The good immobilization properties of S-BL-PC were explored as active phase of a urease biosensor. In order to develop a compact biosensing device, the enzyme-containing solid was

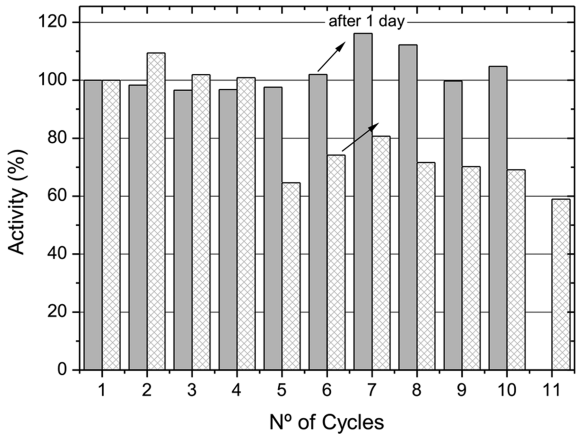

Figure 9. Catalytic activity of COx bioreactors as function of number of catalytic cycles. S-ML-PC (filled columns) and S-BL-PC (checked columns) were loaded with 53 μg COx per mg of support. After each catalytic cycle, the bioreactor was separated and the supernatant was subjected to analysis. Before starting a subsequent cycle, the bioreactors were washed in PB.

dispersed in PVA and spread on the surface of a DTNB modified gold electrode, leading to the formation of a film by solvent casting. The enzyme-modified sensor was immersed in 10 mM PB at pH 7.4 and a peak shift was produced almost instantaneously reaching a constant value after 60−70s (Figure 8a). The short response time, being an important biosensor characteristic, is ascribed to fast enzyme kinetics enabled by good immobilization at the S-BL-PC interface. It also indicates significant diffusivity of both the substrate and the products of the urea conversion through the PVA film. The pH change produced within the confined space of the biohybrid-PVA film is in close proximity to the DTNB-modified electrode surface. Therefore, urea is fast detectable and allows high sensitivity (30.8 ± 0.7 VM^{-1}). For shelf-life time investigation, the urease-biohybrid was kept as dry powder at 4 °C. Enzymatic activity could be maintained up to six months without significant decay of sensitivity (Figure 8b), indicating a very good storage performance.

Interference with electrochemically active substances present in blood serum or urine was tested with ascorbic acid (AA) as one of the most important interferents.[73] AA may affect the signal of the urease-based sensor by two different ways. First, the oxidation peak of ascorbic acid appears at a positive potential around 350 mV at pH 7.4 which does partially overlap with the redox couple of DTNB (data not shown). Second, oxidation products of AA are dehydro-L-ascorbic acid and hydronium ions which will locally decrease the pH. This will lead to a shift of the pH sensitive DTNB redox couple toward positive potentials and thus, counteracting the negative potential shift caused by urea conversion. The initial potential produced by addition of 2 mM urea (referred to as 100% response) is practically unaffected with 0.1 mM AA, and reduced by only 2.6% in the presence of 0.25 mM AA (see the Supporting Information, Figure S6). The physiological level of AA in serum however is only 0.05 mM.[74] This demonstrates that the observed interferences are rather low. The reason is that the PVA layer acts as permselective barrier. This follows a widely used strategy to avoid interferences by limiting the access of electrochemically active substances to the electrode surface.[75,76]

Cholesterol-Bioreactor. The results of the COx activity assays promoted the application of sepiolite-lipid biohybrids (mono- and bilayer) as possible candidates for COx bioreactors. The hybrids contained 53 μg/mg COx, corresponding to 100% uptake, and the bioreactors were dispersed in PB following a stirred batch reactor setup. Figure 9 shows the catalytic activity of these bioreactors as a function of the number of catalytic cycles. It can be noted that the activity of COx after 10 cycles is still very high: 100% on the lipid monolayer and around 60% on the bilayer. Another important characteristic is resistance against mechanical stress. Therefore, after cycle #4, both bioreactor suspensions were vigorously vortexed. As it can be observed from the activity of the subsequent cycle, COx immobilized on S-ML-PC did not show any sign of denaturation while in case of S-BL-PC, the activity decayed by 35%. Furthermore, a recovery effect of the enzyme activity can be observed after storage of both materials for one night in PB at 4 °C. This behavior can be explained by reorganization and conformational changes of the enzyme if immobilized on a support, which provides sufficient mobility. Therefore, this observation can be interpreted as indication of the good biocompatible nature of the sepiolite-supported lipid layers.

CONCLUSIONS

We reported the preparation and structural characterization of various bio-organic interfaces, consisting in different PC based membranes adsorbed on the microfibrous silicate sepiolite. The layers showed important differences in terms of packing density, hydrophilicity, and surface potential. The cytoplasmic enzyme urease and the membrane-associated enzyme cholesterol oxidase were immobilized at these interfaces to probe their biomimetic properties. The preserved enzymatic activity was evaluated with respect to the physicochemical properties of the layers. Both enzymes showed the highest activity on the supported BL-PC membrane as could be expected because this interface resembles the native immobilization environment of URE and COx. Urease associates peripherically, whereas COx binds cooperatively with the aid of an inserted side loop. This association mode is on the other prepared interfaces less possible, which is eventually reflected in the lower enzymatic activity. On the hydrophobic ML-PC and CTA interfaces, induced enzyme orientation may limit substrate access and additionally, severe protein degradation is assumed to occur. These results emphasize the importance of a suitable interface for gentile immobilization.

The excellent enzyme stabilization properties of the sepiolite supported lipid matrices were explored for the construction of urea sensors and cholesterol bioreactors. The immobilized urease retained its activity over several months which can be economically significant. Similarly, the COx-biocatalysts were recyclable under conservation of elevated enzymatic activity. The good dispersion properties of the sepiolite fibers additionally contributed to a homogeneously mixed reaction media offering a large accessible surface area that affords high exploitation of the enzymatic activity and thus high conversion rates.

ASSOCIATED CONTENT

Supporting Information. Additional data showing the calibration curve of a DTNB-modified Au electrode, a discussion of water sorption data, spectra of IR amide bands, data revealing long-term stability of the immobilized enzymes URE and COx, and electrochemical interference with ascorbic acid. This material is available free of charge via the Internet at http://pubs.acs.org/

AUTHOR INFORMATION

Corresponding Author

*Address: Instituto de Ciencia de Materiales de Madrid, CSIC, c/ Sor Juana Inés de la Cruz, 3, Cantoblanco, 28049 Madrid, Spain. Tel: +34 91 334 9000. Fax: +34 91 372 0623. E-mail: eduardo@icmm.csic.es.

ACKNOWLEDGMENT

This work was partially supported by the CICYT (Spain; MAT2009-09960) and the CSIC (Spain; PIF08-018). B.W. acknowledges the Comunidad de Madrid for a *Personal Investigador de Apoyo* contract. We thank Dr. Pedro Tartaj for providing the Zetasizer to conduct the dynamic light scattering measurements.

REFERENCES

(1) *Enzyme Biocatalysis: Principles and Applications*; Illanes, A., Ed.; Springer: Amsterdam, The Netherlands, 2008.

(2) Cracknell, J. A.; Vincent, K. A.; Armstrong, F. A. *Chem. Rev.* **2008**, *108*, 2439.

(3) Girard-Egrot, A. P.; Godoy, S.; Blum, L. J. *Adv. Colloid Interface Sci.* **2005**, *116*, 205.

(4) Yu, A.; Gentle, I.; Lu, G.; Caruso, F. *Chem. Commun.* **2006**, 2150.

(5) Yu, J.; Ge, L.; Dai, P.; Ge, S.; Liu, S. *Biosens. Bioelectron.* **2010**, *25*, 2065.

(6) Onda, M.; Ariga, K.; Kunitake, T. *J. Biosci. Bioeng.* **1999**, *87*, 69.

(7) Siqueira, J. R., Jr; Caseli, L.; Crespilho, F. N.; Zucolotto, V.; Oliveira, O. N., Jr *Biosens. Bioelectron.* **2010**, *25*, 1254.

(8) Oda, I.; Hirata, K.; Watanabe, S.; Shibata, Y.; Kajino, T.; Fukushima, Y.; Iwai, S.; Itoh, S. *J. Phys. Chem. B* **2006**, *110*, 1114.

(9) Ariga, K.; Ji, Q.; Hill, J. *Adv. Polym. Sci.* **2010**, *229*, 51.

(10) Gill, I.; Ballesteros, A. *Trends Biotechnol.* **2000**, *18*, 282.

(11) Avnir, D.; Coradin, T.; Lev, O.; Livage, J. *J. Mater. Chem.* **2006**, *16*, 1013.

(12) Wang, Y.; Caruso, F. *Chem. Mater.* **2005**, *17*, 953.

(13) Ruiz-Hitzky, E.; Darder, M.; Aranda, P.; Ariga, K. *Adv. Mater.* **2010**, *22*, 323.

(14) Bensaude-Vincent, B.; Arribart, H.; Bouligand, Y.; Sanchez, C. *New J. Chem.* **2002**, *26*, 1.

(15) Ariga, K.; Hill, J. P. *Chem. Rec.* **2011**, *11*, 199.

(16) Ramsden, J. J. *Biosens. Bioelectron.* **1998**, *13*, 593.

(17) Darder, M.; Casero, E.; Pariente, F.; Lorenzo, E. *Anal. Chem.* **2000**, *72*, 3784.

(18) Gutierrez-Sanchez, C.; Olea, D.; Marques, M.; Fernandez, V. M.; Pereira, I. A. C.; Velez, M.; de Lacey, A. L. *Langmuir* **2011**, *27*, 6449.

(19) Leidheiser, H.; Deck, P. D. *Science* **1988**, *241*, 1176.

(20) Sackmann, E. *Science* **1996**, *271*, 43.

(21) Groves, J. T.; Dustin, M. L. *J. Immunol. Methods.* **2003**, *278*, 19.

(22) Nikolelis, D. P.; Hianik, T.; Nikoleli, G.-P. *Electroanalysis* **2010**, *22*, 2747.

(23) Rapuano, R.; Carmona-Ribeiro, A. M. *J. Colloid Interface Sci.* **1997**, *193*, 104.

(24) Sanchez-Verdejo, T.; Undabeytia, T.; Nir, S.; Villaverde, J.; Maqueda, C.; Morillo, E. *J. Agric. Food Chem.* **2008**, *56*, 10192.

(25) Begu, S.; Aubert-Pouessel, A.; Polexe, R.; Leitmanova, E.; Lerner, D. A.; Devoisselle, J. M.; Tichit, D. *Chem. Mater.* **2009**, *21*, 2679.

(26) Wicklein, B.; Darder, M.; Aranda, P.; Ruiz-Hitzky, E. *Langmuir* **2010**, *26*, 5217.

(27) Aranda, P.; Fernandes, F. M.; Wicklein, B.; Ruiz-Hitzky, E.; Hill, J. P.; Ariga, K. In *Bioinspiration and Biomimicry in Chemistry*; Swiegers, G. F., Ed.; John Wiley and Sons: Hoboken, NJ, 2012; chapter 5.

(28) Ruiz-Hitzky, E.; Aranda, P.; Serratosa, J. M. In *Handbook of Layered Materials*; Auerbach, S. M., Carrado, K. A., Dutta, P. K., Eds.; Marcel Dekker: New York, 2004; chapter 3.

(29) Krajewska, B. *J. Mol. Catal. B: Enzym.* **2009**, *59*, 9.

(30) Kreit, J.; Sampson, N. S. *Febs J.* **2009**, *276*, 6844.

(31) Nauck, M.; Marz, W.; Wieland, H. *Clin. Chem.* **2000**, *46*, 436.

(32) Dubois, M.; Gilles, K.; Hamilton, J. K.; Rebers, P. A.; Smith, F. *Nature* **1951**, *168*, 167.

(33) Aranda, P.; Kun, R.; Martín-Luengo, M. A.; Letaïef, S.; Dékány, I.; Ruiz-Hitzky, E. *Chem. Mater.* **2008**, *20*, 84.

(34) Bradford, M. M. *Anal. Biochem.* **1976**, *72*, 248.

(35) Casero, E.; Darder, M.; Takada, K.; Abruna, H. D.; Pariente, F.; Lorenzo, E. *Langmuir* **1999**, *15*, 127.

(36) Knapp, C.; Gil-Llambias, F. J.; Gulppi-Cabra, M.; Avila, P.; Blanco, J. *J. Mater. Chem.* **1997**, *7*, 1641.

(37) Ruiz-Hitzky, E. *J. Mater. Chem.* **2001**, *11*, 86.

(38) Alkan, M.; Demirbas, O.; Dogan, M. *J. Colloid Interface Sci.* **2005**, *281*, 240.

(39) Savarala, S.; Ahmed, S.; Ilies, M. A.; Wunder, S. L. *Langmuir* **2010**, *26*, 12081.

(40) Chibowski, E.; Delgado, A. V.; Rudzka, K.; Szczes, A.; Holysz, L. *J. Colloid Interface Sci.* **2011**, *353*, 281.

(41) Zimmermann, R.; Kuttner, D.; Renner, L.; Kaufmann, M.; Zitzmann, J.; Muller, M.; Werner, C. *Biointerphases* **2009**, *4*, 1.

(42) Chang Chung, Y.; Hong Chiu, Y.; Wei Wu, Y.; Tai Tao, Y. *Biomaterials* **2005**, *26*, 2313.

(43) Giles, C. H.; D'Silva, A. P.; Easton, I. A. *J. Colloid Interface Sci.* **1974**, *47*, 766.

(44) Kumar, N.; Garo, S.; Tilton, R. D. *Langmuir* **2004**, *20*, 4446.

(45) Shinoda, K.; Yamaguchi, T.; Hori, R. *Bull. Chem. Soc. Jpn.* **1961**, *34*, 237.

(46) Zhou, Q.; Somasundaran, P. *J. Colloid Interface Sci.* **2009**, *331*, 288.

(47) Persson, C. M.; Claesson, P. M.; Lunkenheimer, K. *J. Colloid Interface Sci.* **2002**, *251*, 182.

(48) Gu, T.; Rupprecht, H. *Colloid Polym. Sci.* **1990**, *268*, 1148.

(49) Darder, M.; Casero, E.; Diaz, D. J.; Abruña, H. D.; Pariente, F.; Lorenzo, E. *Langmuir* **2000**, *16*, 9804.

(50) Dick, S. G.; Fuerstenau, D. W.; Healy, T. W. *J. Colloid Interface Sci.* **1971**, *37*, 595.

(51) Waltermo, Å.; Claesson, P. M.; Johansson, I. *J. Colloid Interface Sci.* **1996**, *183*, 506.

(52) Park, G. S. In *Synthetic Membranes: Science, Engineering. and Applications*; Bungay, P. M., Lonsdale, H. K., de Pinho, M. N., Eds.; Reidel: Dordrecht, The Netherlands, 1986; chapter 2, p 57.

(53) Birch, W. R.; Knewtson, M. A.; Garoff, S.; Suter, R. M.; Satija, S. *Colloids Surf., A* **1994**, *89*, 145.

(54) Cesareo, S. D.; Langton, S. R. *Fems Microbiol. Lett.* **1992**, *99*, 15.

(55) Vial, S.; Prevot, V.; Leroux, F.; Forano, C. *Microporous Mesoporous Mater.* **2008**, *107*, 190.

(56) Wang, C.; Ye, F.; Valardez, G. F.; Peters, G. H.; Westh, P. *J. Phys. Chem. B* **2011**, *115*, 196.

(57) Andrews, A. T. *Electrophoresis: Theory, Techniques and Biomedical and Clinical Applications*, 2 ed.; Oxford University Press: New York, 1986; p 7.

(58) Remaut, H.; Safarov, N.; Ciurli, S.; Van Beeumen, J. *J. Biol. Chem.* **2001**, *276*, 49365.

(59) Hou, Y.; Jaffrezic-Renault, N.; Zhang, A.; Wan, J.; Errachid, A.; Chovelon, J. M. *Sens. Actuators, B* **2002**, *86*, 143.

(60) Chen, X. Y.; Wolfgang, D. E.; Sampson, N. S. *Biochemistry* **2000**, *39*, 13383.

(61) Ferraz, H. C.; Guimaraes, J. A.; Alves, T. L. M.; Constantino, C. J. L. *Appl. Surf. Sci.* **2011**, *257*, 6535.

(62) Wildgoose, G. G.; Pandurangappa, M.; Lawrence, N. S.; Jiang, L.; Jones, T. G. J.; Compton, R. G. *Talanta* **2003**, *60*, 887.

(63) Streeter, I.; Leventis, H. C.; Wildgoose, G. G.; Pandurangappa, M.; Lawrence, N. S.; Jiang, L.; Jones, T. G. J.; Compton, R. G. *J. Solid State Electrochem.* **2004**, *8*, 718.

(64) Kurganov, B. I.; Lobanov, A. V.; Borisov, I. A.; Reshetilov, A. N. *Anal. Chim. Acta* **2001**, *427*, 11.

(65) Azari, F.; Hosseinkhani, S.; Nemat-Gorgani, M. *Appl. Biochem. Biotechnol.* **2001**, *94*, 265.

(66) Baron, C.; Thompson, T. E. *Biochim. Biophys. Acta* **1975**, *382*, 276.
(67) Stubbs, G. W.; Smith, H. G.; Litman, B. J. *Biochim. Biophys. Acta* **1976**, *426*, 46.
(68) Magaña-Plaza, I.; Montes, C.; Ruiz-Herrera, J. *Biochim. Biophys. Acta* **1971**, *242*, 230.
(69) Bunting, P. S.; Laidler, K. J. *Biochemistry* **1972**, *11*, 4477.
(70) Hamilton, B. K.; Stockmeyer, L. J.; Colton, C. K. *J. Theor. Biol.* **1973**, *41*, 547.
(71) Kato, K.; Walde, P.; Mitsui, H.; Higashi, N. *Biotechnol. Bioeng.* **2003**, *84*, 415.
(72) Kouassi, G.; Irudayaraj, J.; McCarty, G. *J. Nanobiotechnol.* **2005**, *3*, 1.
(73) Mizutani, F.; Yabuki, S.; Sato, Y. *Biosens. Bioelectron.* **1997**, *12*, 321.
(74) Mizutani, F.; Sato, Y.; Sawaguchi, T.; Yabuki, S.; Iijima, S. *Sens. Actuators, B* **1998**, *52*, 23.
(75) Vaidya, R.; Wilkins, E. *Electroanal* **1994**, *6*, 677.
(76) Madaras, M. B.; Buck, R. P. *Anal. Chem.* **1996**, *68*, 3832.